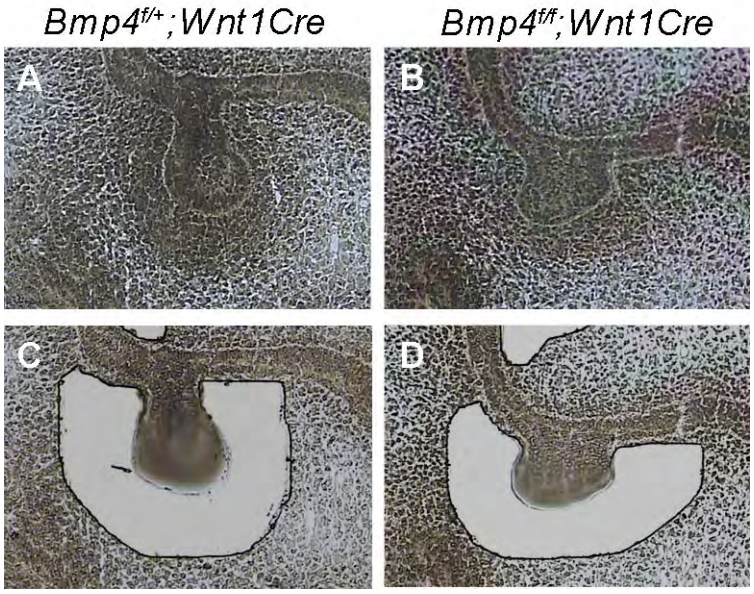

Fig. S1. Representative images of sections of E13.5 first molar tooth germs before and after LCM isolation of tooth mesenchyme. (**A**,**C**) *Bmp4$^{f/+}$;Wnt1Cre* control samples. (**B**,**D**) *Bmp4$^{f/f}$;Wnt1Cre* mutant samples.

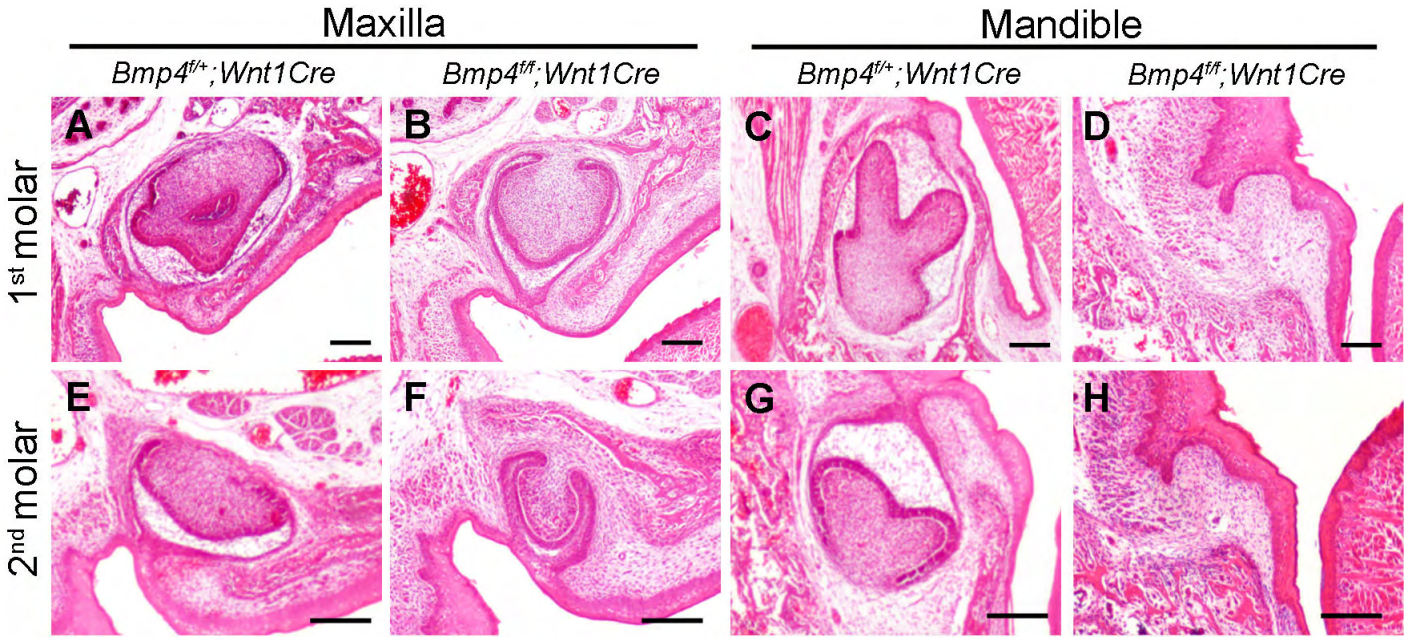

Fig. S2. *Bmp4$^{f/f}$Wnt1Cre* mutant mice exhibit developmental arrest of mandibular molar and delayed development of maxillary molar tooth germs. (**A-D**) Hematoxylin and Eosin-stained frontal sections through the first molar tooth germs of P0 control and mutant mice. (**E-H**) Hematoxylin and Eosin-stained frontal sections through the second molar tooth germs of control and mutant mice. Scale bars: 50 μm.

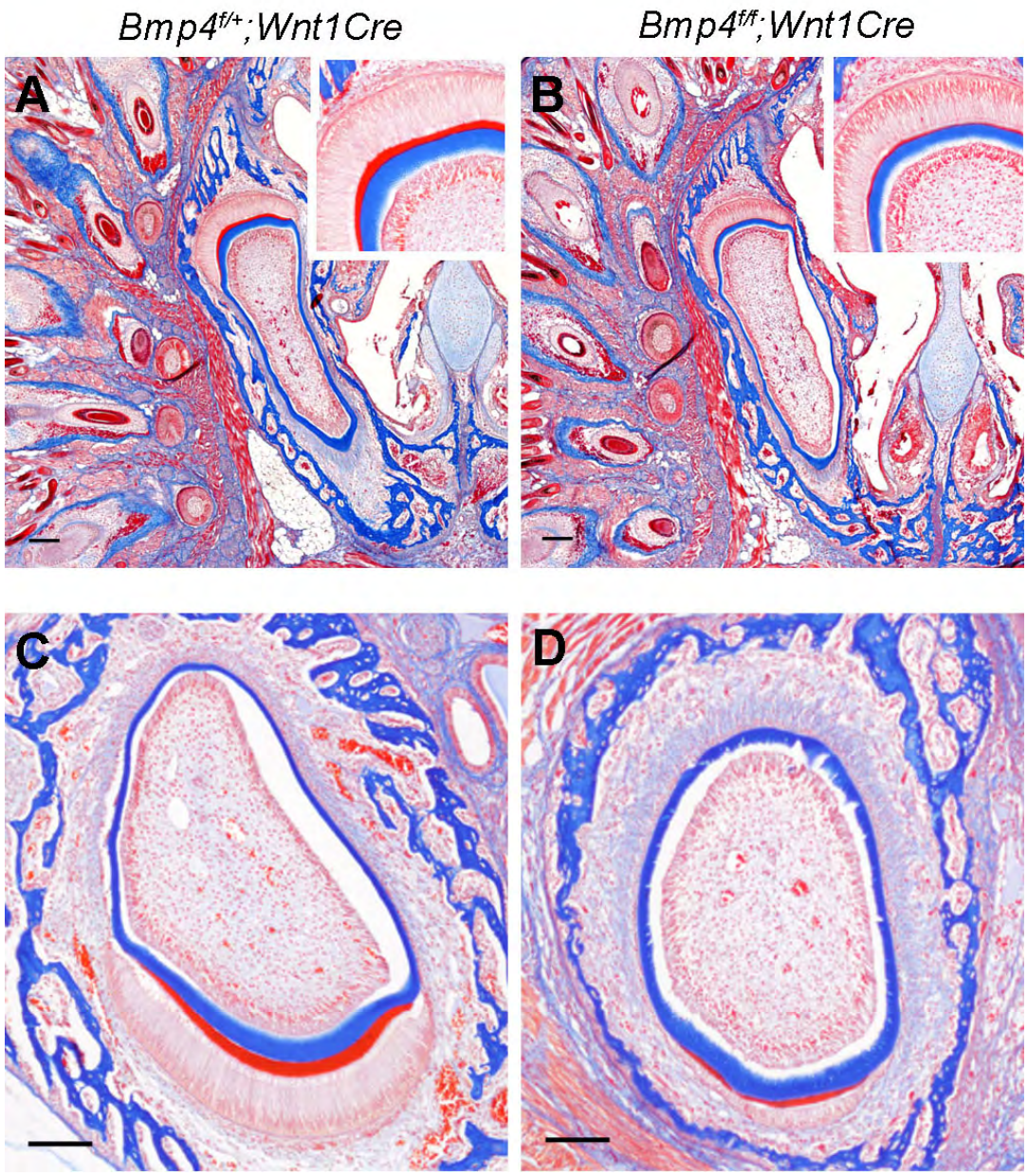

Fig. S3. Histological analyses of incisor defects in the *Bmp4$^{f/f}$;Wnt1Cre* mutant mice. Frontal sections of P5 mice were assayed by trichrome staining. The enamel matrix was stained red and dentin matrix blue. (**A**,**B**) The upper incisors. The inset at the upper-right corner of the panel shows higher magnification view of the ameloblast and odontoblast layers at the labile side of the tooth germ. (**C**,**D**) The lower incisors. The mutant lower incisor (D) was more rounded and had thinner enamel layer on the labile surface than that in the control littermate (C). Scale bars: 100 μm.

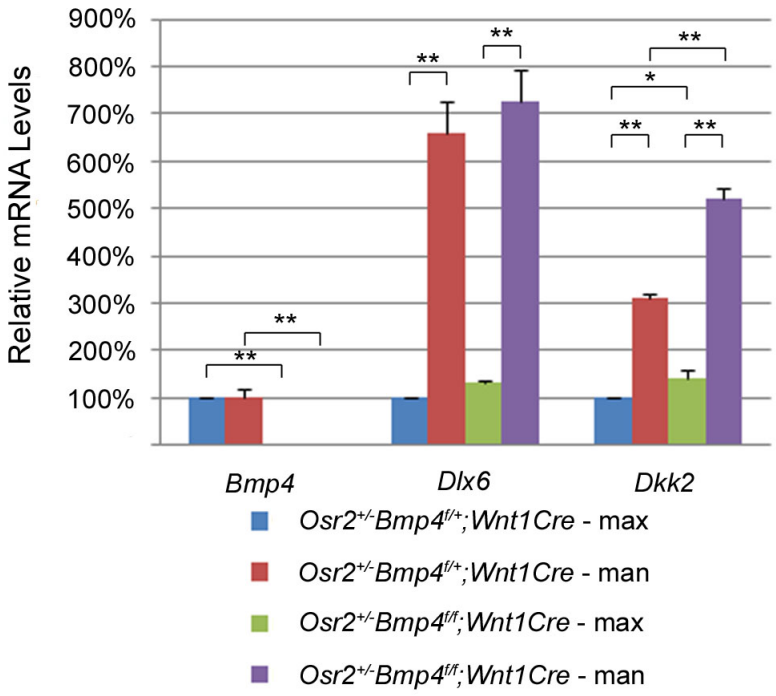

Fig. S4. Relative levels of *Bmp4*, *Dlx6* and *Dkk2* mRNAs, respectively, in the maxillary and mandibular molar mesenchyme in control and *Osr2*$^{+/-}$*Bmp4*$^{f/f}$*;Wnt1Cre* mutant embryos. **P*<0.05, ***P*<0.01.

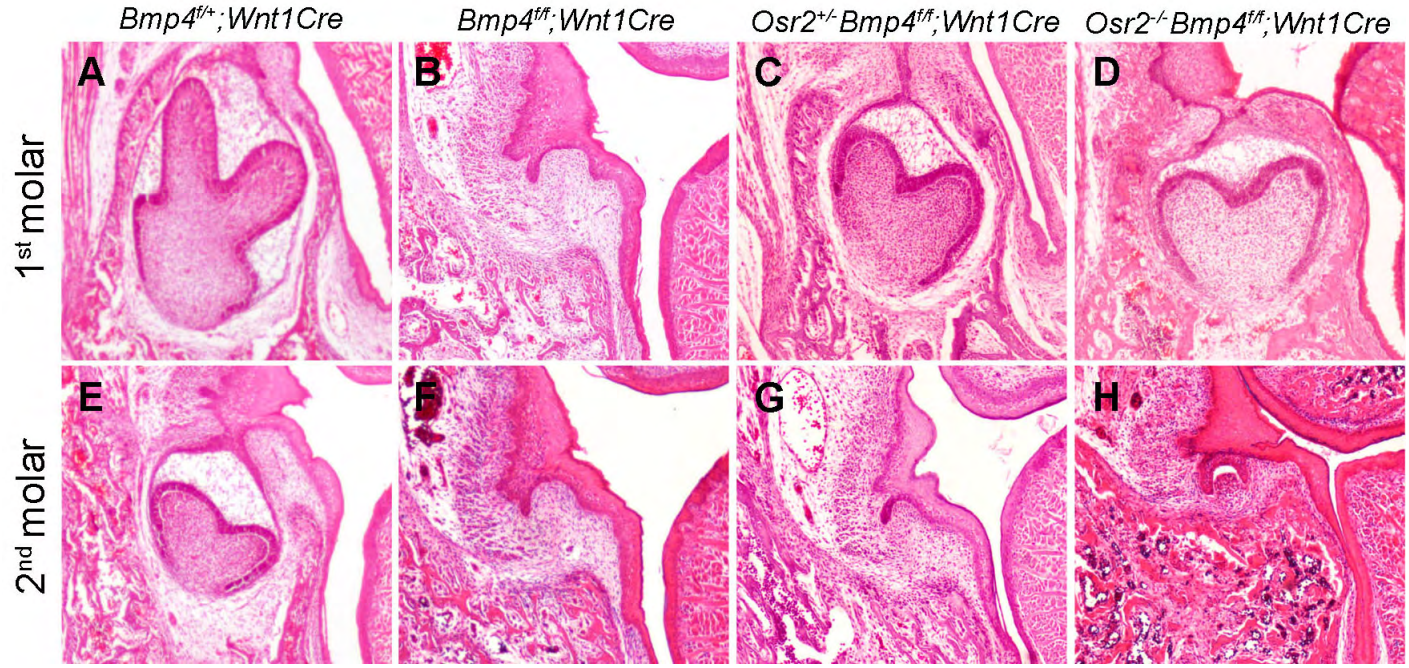

Fig. S5. Mandibular molar development in the *Osr2*$^{-/-}$*Bmp4*$^{f/-}$*;Wnt1Cre* compound mutant mice. (**A-D**) Hematoxylin and Eosin-stained frontal sections through the developing mandibular first molar tooth germs of *Bmp4*$^{f/+}$*;Wnt1Cre* (A), *Bmp4*$^{f/f}$*;Wnt1Cre* (B), *Osr2*$^{+/-}$*Bmp4*$^{f/-}$*;Wnt1Cre* (C) and *Osr2*$^{-/-}$*Bmp4*$^{f/-}$*;Wnt1Cre* (D) mutant pups at P0. (**E-H**) Hematoxylin and Eosin-stained frontal sections through the developing mandibular second molar tooth germs of *Bmp4*$^{f/+}$*;Wnt1Cre* (E), *Bmp4*$^{f/f}$*;Wnt1Cre* (F), *Osr2*$^{+/-}$*Bmp4*$^{f/-}$*;Wnt1Cre* (G) and *Osr2*$^{-/-}$*Bmp4*$^{f/-}$*;Wnt1Cre* (H) mutant pups at P0.

Table S1. RNAseq read densities of each of the *Bmp4* exons

Exon	Ctr-max (RPM)	Ctr-man (RPM)	mt-max (RPM)	mt-man (RPM)
4	29.98	30.46	0.21 (0.7%)*	0.18 (0.6%)*
3	3.96	4.92	4.31	4.46
2	1.08	1.51	1.56	2.20
1	1.63	2.08	2.30	2.62

RPM, reads per million mapped reads.
*$P<0.01$ for comparison between control and mutant samples. No significant difference is detected between the maxillary and mandibular molar mesenchyme in either control or mutant samples.

Table S2. RNAseq results for Bmp family ligands

Gene	Ctr-max (RPKM)	Ctr-man (RPKM)	mt-max (RPKM)	mt-man (RPKM)
Bmp2	2.02	4.31	2.26	7.87
Bmp3	17.40	11.84	8.52	4.57
Bmp5	2.60	1.66	0.18	0.10
Bmp6	35.49	33.82	46.73	26.88
Bmp7	3.46	3.38	7.45	4.99
Bmp8a	0.00	0.02	0.00	0.00
Bmp8b	0.57	0.84	0.18	0.40
Bmp10	0.00	0.00	0.00	0.00
Bmp15	0.10	0.00	0.18	0.29

RPKM, reads per kilobase exon per million mapped sequences.

Table S3. Expression profiles of selected genes in maxillary and mandibular mesenchyme

Gene	Ctr-Max	Mt-Max	Ctr-Man	Mt-Man	Ctr-Man vs Ctr-Max		Mt-Max vs Ctr-Max		Mt-Man vs Ctr-Man	
					FC	*P*-value	FC	*P*-value	FC	*P*-value
Dlx6	4.48	3.81	19.78	17.2	4.42	4.36E–07	–1.18	0.65	–1.15	0.67
Wif1	5.52	5.4	13.29	15.72	2.41	8.86E–06	–1.02	0.90	1.18	0.42
Dkk2	9.52	16.37	34.22	63.52	3.59	1.90E–38	1.72	1.23E–04	1.86	5.02E–23
Osr2	92.42	124.03	110.33	177.91	1.19	0.13	1.34	1.81E–05	1.61	5.74E–19

The expression levels shown are in RPKM.
–, downregulation; FC, fold change.